Elsevier Editorial System(tm) for Chemosphere

Manuscript Draft

Manuscript Number:

Title: UV characterization and photodegradation mechanism of the fungicide chlorothalonil in the presence and absence of oxygen

Article Type: Research paper

Section/Category: Environmental Chemistry (including Persistent Organic Pollutants and Dioxins)

Keywords: Vibrationally resolved UV-Vis spectrum
Photodegradation
Chlorothalonil

Corresponding Author: Professor Gustavo Argüello, Dr.

Corresponding Author's Institution: INFIQC - Universidad Nacional de Córdoba-Facultad de Ciencias Químicas

First Author: Maria V Cooke, Bachellor

Order of Authors: Maria V Cooke, Bachellor ; María B Oviedo; Walter J Peláez; Gustavo Argüello, Dr.

Suggested Reviewers: María DoSantos Afonso
Departamento de Química Inorgánica y Química Física, Universidad de Buenos Aires
mdsafonso@gmail.com; dosantos@qi.fcen.uba.ar
She is a physical chemist with expertise in photochemistry and environmental chemistry

Esther Oliveros
Institut de Chimie de Toulouse , Université Paul Sabatier - Toulouse
oliveros@chimie.ups-tlse.fr
Leading scientist in environmental chemistry and photochemistry

Graciela Arbilla
Instituto de Química, Universidade Federal do Rio de Janeiro
graciela@iq.ufrj.br; gracielaiq@gmail.com
Head of the laboratory of atmospheric chemistry and pollution of the University of Sao Paulo

Fernando García Einschlag
Departamento de Química - Fac. de Ciencias Exactas, Universidad Nacional de La Plata
fgarciae@quimica.unlp.edu.ar
Expertise on the treatment of contaminants through the use of advanced oxidation processes

Marie E DeLorenzo
Center for Coastal Environmental Health and Biomolecular Research, NOAA, National Ocean Service

marie.delorenzo@noaa.gov
Leading scientist in environmental chemistry

Frank Wania
Departmento of Physical and Environmental Sciences, University of Toronto
frank.wania@utoronto.ca
Leading scientist in Environmental chemistry

*Cover Letter

Universidad Nacional de Córdoba
INFIQC - Departamento de Fisicoquímica - Facultad de Ciencias Químicas
Ciudad Universitaria - X5000HUA Córdoba - Argentina

Dr. Jacob de Boer (Editor)
Chemosphere

February, the 13th, 2017

Dear Dr.

We hereby submitt in electronic form our article "UV characterization and photodegradation mechanism of the fungicide chlorothalonil in the presence and absence of oxygen" by Cooke, Oviedo, Peláez and myself to be considered for publication as an Article in Chemosphere.
We believe that the present contribution should be of onterest to a broad range of scientists working in the areas of Photochemistry, Kinetics and Toxicology since the subject of our article deals with the widespread distributed pesticide chlorothalonil.
We really thank you in advance for your consideration of our manuscript and shall be looking forward to hearing from you.
Sincerely,

Prof. Dr. Gustavo A. Argüello

Corresponding author: Gustavo A. Argüello
Name: Gustavo A. Argüello
Address: INFIQC, Dpto de Físico Química, Facultad de Ciencias Químicas, Universidad Nacional de Córdoba, Ciudad Universitaria. X5000HUA Córdoba, Argentina
Phone: + 54 351 433 4169
Fax: + 54 351 433 4188
e-mail: gaac.isea@gmail.com

Highlights

Franck-Condon resolved UV-Vis spectrum of Chlorothalonil

Photolysis and isomer speciation

Pesticide degradation pathways

UV characterization and photodegradation mechanism of the fungicide chlorothalonil in the presence and absence of oxygen

María Victoria Cooke,[a] María Belén Oviedo,[b] Walter José Peláez [a] and Gustavo Alejandro Argüello [a]

[a] INFIQC-CONICET-Dpto. de Fisicoquímica, Facultad de Ciencias Químicas, Universidad Nacional de Córdoba, Ciudad Universitaria, Córdoba, X5000HUA, Argentina.

[a] INFIQC-CONICET-Dpto. de Química Teórica y Computacional, Facultad de Ciencias Químicas, Universidad Nacional de Córdoba, Ciudad Universitaria, Córdoba, X5000HUA, Argentina.

Corresponding Author: gaac@fcq.unc.edu.ar

Abstract

An experimental and theoretical study of the UV spectrum of CT was carried out and the vibrationally resolved HOMO→LUMO transition is presented for the first time. The fluorescence spectrum has also been recorded. Furthermore, preparative photolysis in acetonitrile allowed a detailed study of the photoproducts formed with recognition of different isomers. In the presence of oxygen only the first reductive dechlorination-decyanation occurred, while in its absence a successive dechlorination-decyanation takes place.

Graphical Abstract

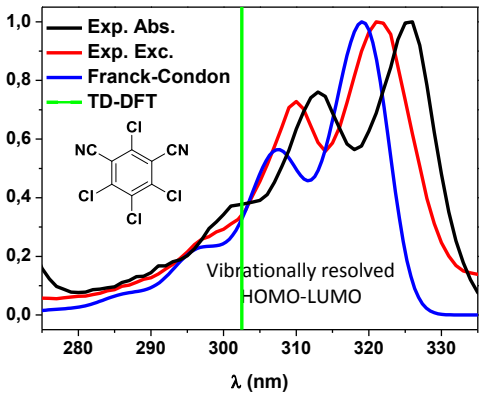

Highlights

Franck-Condon resolved UV-Vis spectrum of Chlorothalonil

Photolysis and isomer speciation

Pesticide degradation pathways

Keywords

Vibrationally resolved UV-Vis spectrum

Photodegradation

Chlorothalonil

1. Introduction

Chlorothalonil (CT, **1**) is a frequently used broad spectrum organochlorine non-systemic foliar fungicide employed in the prevention and control of fungal diseases (especially in agricultural crops and other commodities) as well as a preservative of paints, resins, emulsions, etc.[1,2] In 1997, almost 6000 Tons were used in the US in the control of grains, peanuts and potatoes[3] and in 2014 600 Tons were employed in California alone. The exponential growth of worldwide CT usage is due to its high efficacy as an antifungal, which is attributed to the thiol moiety inactivation in proteins such as glutathione and Coenzyme A. [4-5]

Most commercial brands declare that CT is highly toxic to fish; however it is claimed to have low toxicity to the wildlife. The legal dispositions regarding the usage of this active constituent applied in Argentina[6] classify CT as a type IV fungicide, usually causing no harm when applied as it is established for each crop. Nevertheless, the damage that can be caused by the residual fungicide (that usually ends up in water bodies) through bioaccumulation is still unknown. Besides, it has been classified as a probable human carcinogen.[7] Therefore, a thorough and comprehensive knowledge of all its chemistry appears to be necessary. There have been many studies on photolysis of chlorothalonil; already in 1988 Millet at al.[8] informed that the persistence in the environment varied between 22 and 200 days (summer and winter conditions), while Peñuela et al. concluded that it is stable to UV light in aqueous media and in the crystalline state that degrades mainly through dechlorination and partly through a substitution reaction[9]. Kwon et al.[10] treated the partitioning of chlorothalonil between water and sediments and also reported the formation of dehydrochlorination products with 4-hydroxy as the main product; Tan et al.,[11] in turn studied the nanometer photosensitizing TiO_2 particles effect in aqueous media encountering complete degradation and no presence of the intermediate 4-hydroxy.

Also photolysis has been studied in solvents other than water [benzene,[12] dichloromethane,[13] ethanol,[14-15] methanol,[15-16] thin paraffin wax films –representing the upper layers of leafs- and n-heptane[17]] with varying results but an underlying recognition that dechlorination is the main degradation mechanism. Though for some of the papers cited, there is no explicit mentioning of the wavelengths used, it can be concluded that all of them used solar radiation or solar substitutes. Finally, the most recent paper by Bouchama et al.[18] that studied the photolysis in water/acetonitrile made

an elegant contribution, not only by measuring the transient species occurring in the photo-degradation and concluding that the first step of the reaction is the formation of the triplet excited state of CT with a high capacity to generate singlet oxygen by energy transfer, but by recognizing that CT photolysis is far from being understood. This leaves open the race to new efforts such as the present study that aims to analyze and comprehend: a) the transitions involved in the UV spectrum of CT; b) the reactions when photolysis is carried out beyond the surface´s wavelength range; c) the measurement of its fluorescence when excited with short wavelength radiation, and d) the unraveling of the photoproducts produced.

We previously reported the photochemical degradation of trifluoralin[19] another widely used pesticide that decomposes by action of UV-Vis light into several products for which there are no studies about their properties as also happens for many of the products of CT.[15] Besides, another contribution has been made[20] with calculations of UV absorption bands and their intensities in the spectra of some tetrahydroquinolines that apply for the present study.

2. Materials and Methods

2.1. Materials

CT (99.2%) was supplied by Riedel-de Haen. For the preparative photolyses CT was purified from a commercial sample (compressed powder 82.5% p/p) via ethyl acetate solvent extraction, followed by column chromatography using a solvent mixture of n-hexane and dichloromethane. L-cystine was synthesized using L-cysteine (>97%) provided by Sigma-Aldrich and hydrogen peroxide (Cicarelli, 30% solution) in an acidic medium. Tris(2,2'-bipyridine)-ruthenium(II) chloride from Sigma was used as the fluorescence quantum yield standard. Acetonitrile (ACN, HPLC 99.5%) was provided by Sintorgan. Ethanol (99.8%) was provided by Merck. Water was purified using a reverse osmosis RIOS 5 and Synergy (Millipore) (resistivity 18.2 MΩ cm, DOC < 0.1 mg L^{-1}). All solvents and chemicals were used as received.

2.2. Irradiation methods

Irradiation was conducted using four low pressure mercury lamps emitting at 254 nm. For the product analysis, the CT solutions in ACN (4 mM) were placed in a quartz cell and purged with O_2 or N_2 for 30 minutes before irradiation. For all the systems a solvent trap was placed to reduce the loss via evaporation. Afterwards, as the solution was still connected to the O_2/N_2 flow, it was irradiated for 2 hours. A preparative photolysis of CT with a N_2 purge was done for 48 hs to establish the identity of the different isomers of the photoproducts and it was analyzed at different times via GC-MS to obtain a relative profile of the disappearance of CT and the appearance of its photoproducts. Although a total isolation of the photoproducts was not achieved via preparative chromatography, the analysis of the ^{1}H-NMR and the GC-MS spectra of the different fractions obtained allowed us to identify several isomers of the photoproducts.

For the determination of the formation of $^1O_2$ during the photolysis of CT, a solution of CT (1.5 mM)/L-cysteine (16.5 mM) was prepared in ACN:H_2O (60:40), since the solubility of L-cysteine in ACN is very low. This solution was irradiated for 30 minutes in the presence of O_2. A control in darkness was also performed.

2.3. Experimental Analyses

UV-visible spectra were recorded on an Agilent 8354 spectrophotometer and a quartz cell with an optical path of 1 cm. CT excitation and emission fluorescence spectra were recorded using a PTI QM2 (Quanta Master 2) spectrofluorometer from Photon Technology International which utilizes a pulsed Xe lamp (75 W) as an excitation source and a photon-counting detector. The identification of the photoproducts was conducted with GC-MS analyses performed on a Shimadzu GC-MS-QP 5050 spectrometer. The Column was a non-polar phase (95% dimethylpolysiloxane-5% phenyl), 30 m long and with an internal diameter of 0.25 mm. The elution gas was Helium with a flux of 0.6 mL min^{-1}. The injector and ion source temperature was 280ºC, the oven heating ramp was 15ºC min^{-1} from 150ºC up to 280ºC, and the interface temperature was 300ºC. The pressure in the MS instrument was 10^{-5} Torr, precluding ion-molecule reactions from taking place, and MS recordings were made in the electron impact mode (EI) at an ionization energy of 70 eV. The NMR spectra were obtained with a Bruker Advance II 400 MHz spectrometer (BBI probe, z gradient). The Infrared spectra were acquired on a FTIR-Bruker IFS28 spectrometer, with a resolution of 2 cm^{-1} in a range of 4000 to 400 cm^{-1} using KBr disks.

3. Theoretical Calculations

The molecular structure of (CT) in acetonitrile (ACN) was optimized at the DFT level using Gaussian 09 code.[21] The B3LYP (Becke three-parameter Lee-Yang-Parr)[22,23] exchange correlation functional was employed, and the 6-31+G(d,p) basis set was used for the expansion of the Kohn-Sham orbitals of all the atoms. The polarizable conductor calculation model (CPCM) of solvatation was used in all calculations.[24,25] The gradient threshold for geometry optimization was taken as $4{,}5.10^{-4}$ Hartree/Bohr. At the optimized geometry, time-dependent DFT (TDDFT) calculations, with the same basis set as before was performed to compute the excited-state vertical transition energies and oscillator strengths. In order to check that the optimized geometry corresponds to a minimum in the potential energy surface a frequency analysis at the same level of theory was computed.

For the simulation of the vibrationally resolved electronic spectrum, the methodology of Bloino and Barone was used as implemented in Gaussian 09. The theoretical description used to compute the absorption spectrum has been widely described in refs.[26-28] In summary, this methodology is based on the calculation of the Franck-Condon (FC) integrals, between the vibrational wavefunctions of the electronic states involved in the transition. These integrals are obtained by expanding the electronic transition dipole moment in a Taylor series of the normal coordinates. The zeroth order term corresponds to the Frank-Condon (FC) approximation where the transition dipole moment is unchanged during the transition. The Adiabatic Hessian (AH) model has been applied to study the first two lowest electronic transitions for the CT molecule in ACN. Within this framework, the equilibrium geometry and vibrational structure of both electronic states are required. The normal modes of the initial and final states can be related through a linear transformation proposed by Duschinsky.[29] We have considered the equilibrium solvatation regime for introducing the solvent effect in the electronic transition, where all the solvent degrees of freedom are in equilibrium with the molecule. Theoretical coefficients (ε_{calc}) have been calculated by the formula (1):[30]

$$\varepsilon_{calc} = f\ x\ 2.699\ x\ \frac{10^4}{b}, \quad (1)$$

Where b is the line width and f is the oscillator strength.

4. Results and discussion

4.1. Experimental Characterization

The UV spectrum of CT was recorded in ACN, EtOH and H_2O:ACN (70:30) in order to obtain information about the nature of the transitions involved in the main bands. As the results in the different solvents were similar, the UV spectrum of CT in ACN was taken as representative (see Supp. Inf. for CT in EtOH and H_2O:ACN). It consists of different absorption regions, that we will roughly call the short (200-250 nm), medium (250-280 nm) and long (280-340 nm) wavelength regions (figure 1.a). In the short wavelength region we can observe the most intense band centered at approximately 230 nm with a slight shoulder at lower wavelengths. In the medium wavelength region (figure 1.b) there are two distinct wide bands, the one located at lower wavelengths being more intense. In the long wavelength region (figure 1.c), there are clearly three bands of decreasing intensity towards the high energy region. In this group, the more intense band belongs to the lowest energy.

Seven experimental absorption maxima (which are presented in Table 1 for all the solvents used) where determined with the aid of the second derivative spectra and their respective molar absorption coefficients were obtained. Although we were able to determine each band maxima in different solvents we could not observe a clear shift tendency and therefore were not able to assess, by this method, the nature of the electronic transitions of the absorption bands.

(Figure 1 and Table 1 near here)

4.2. Computational Characterization

Because of that, a different approach was conducted through TD-DFT simulations using the Gaussian 09 program.[21] A geometry optimization of the fundamental state (S_0) of CT in ACN was performed and we obtained a planar structure with C_{2v} symmetry, which corresponds with the established structure.

(Figure 2 near here)

The results of the calculation of the excitation energies of CT in ACN are shown in figure 2 together with the experimental spectrum. The excitation energies, the oscillator strength of each electronic transition as well as the assignments (that were carried out after an analysis of the molecular orbitals that are concerned) are all presented in figure

3. Here, one can readily recognize, through the orbitals involved, that the main electronic excitations are $\pi \rightarrow \pi^*$. The HOMO-2 orbital does not contribute to any electronic transition since it is constricted by symmetry and thus those transitions involving it result as optically inactive.

(Figure 3 near here)

It is seen that the TD-DFT calculations agree with the most prominent observed feature in the short wavelength region of the experimental spectrum with a small red-shift deviation of around 6 nm. Also for the other two transitions there is a close resemblance in terms of both, position and intensity. Even the small shoulder below 230 nm is given a transition in the calculus. Therefore the four bands in the short and medium wavelength regions are reproduced, which is not the case of the single transition given for the long wavelength region. If it were mandatory to rely on calculations, then those three maxima given by the second derivative model should conform only one electronic transition. Given the structural similarity of CT with benzene (after all CT is a fully substituted benzene) and the fine structure shown by its UV spectrum, then the bunch of peaks were investigated by taking into account the vibronic structure using the Franck-Condon approximation.[31,32]

The optimized molecular structure of the first electronic excited state was obtained. The optimization maintains the plane of the molecule with barely any change in the structure (the root mean square deviation for the first excited state geometry is 0.028 Å, which means an almost exact superposition of the atoms). This finding is in accordance with the Franck-Condon principle for vertical excitation. In order to simulate the vibrationally resolved electronic spectrum, we have used the methodology of Bloino and Barone as implemented in Gaussian 09.[21,33] This method has been successfully used to calculate the optical properties of aminocoumarines,[34] anisol-phenol complex,[35] anisol dimer,[36] alizarin pigments[37] and phenyl radical.[38]

(Figure 4 near here)

The vibrationally resolved absorption spectrum for the lowest electronic transition calculated is shown as the blue trace in figure 4. The main shapes and peak location agree with the experimental spectrum (black trace) showing that there is indeed a vibronic element in the long wavelength region, making it an important asset in the knowledge of the nature of the transition that most people have been using for

irradiation to carry out the great majority of the photochemical studies. The figure also shows the agreement with the fluorescence (red trace) excitation spectrum (to be discussed later on) taken at a fixed wavelength for emission. This close resemblance speaks for the reliability of the calculations. Since both states, the fundamental S_0 and the first excited one S_1 have very similar structures, it can be reasonably assumed that the potential energy surfaces will be practically aligned in terms of distances (resulting in true vertical transitions). Then, the most intense vibronic transition will be the 0-0 since the overlapping of wave functions will be the highest. The other transitions seen in the spectrum will correspond to the 0-2 and 0-4 because the odd transitions will all have null integrals. Figure 4 sketches both the observed transitions as well as a representation of their intensities.

4.3. Irradiation with UV light. Kinetics

As it has been said before, practically all the works published were carried out by photolysing with broadband (fluorescent or not) lights in the λ>300 nm wavelength region. We undertook our studies at shorter wavelengths in order to assess whether the change in the electronic transition affects specific features (like for example the ability to generate $^1O_2$), or the identity of the photoproducts. The excitation with a 254 nm photon ends in the second excited state ($S_0 \rightarrow S_2$) (cf. fig. 3).

The experimental arrangement was as follows: a 2×10^{-5} M solution of CT in ACN was irradiated and its decomposition was followed by UV spectroscopy. In figure 5, it can be observed that as the photolysis progresses there is a slight hipsochromic shift in the main UV band. Therefore, the rate of disappearance could only be reliably determined during the first stages of the photolysis. Another interesting fact is that even though at the wavelength of photolysis CT has a considerable molar absorptivity coefficient (table 1), the rate at which CT is being photolized is slow. This effect could be rationalized accounting for all possible reaction paths of the excited state. Among them, the radiative relaxation to the fundamental state in the form of fluorescence is an effective way the molecule has to loose energy without decomposing. We could measure and record the fluorescence spectrum because there was no overlapping between excitation and emission wavelengths (recall that the maximum of fluorescent emission peaks around 355 nm which is the wavelength mostly used by other workers). Nevertheless, the quantum yield determined (measurements relative to $Ru(bpy)_3^{2+}$-with a known quantum

yield)[39] gave values of the order of 10^{-3} (cf. supporting information). The measurement of fluorescence emission at different excitation energies show (see supporting information) that the morphology of the emission is independent of excitation wavelength while the intensities closely follow the pattern shown in figure 4. This is a strong indication that the radiationless relaxation from S_2 to S_1 has already taken place when fluorescence starts and only one excited state is involved in the fluorescence.

(Figure 5 near here)

It has been previously reported that O_2 acts as a quencher of the excited state of CT.[40] For that reason we decided to analyze the kinetics in presence and absence of O_2. The solutions were purged with O_2 or N_2 prior to the photolysis. The main difference of these photolyses is the rate at which CT is disappearing. The analysis of the disappearance rate under the different conditions can be seen in figure 6 were $\ln(A/A_0)$ *vs.* time is represented. The photolysis of CT in O_2 has a lineal decay in time so it can be concluded that the process is of first order. The photolysis of CT in N_2 shows linear behavior only in the first fifty seconds of the photolysis. The overall constants obtained under the different conditions are reported in the inset of fig 6. It can be observed that the rate is almost 30 times greater when there is no oxygen in the medium. This could indicate that the presence of O_2 plays the same role as when the photolysis is carried out at longer wavelengths thus reinforcing the idea of the attainment of the same final excited state.

(Figure 6 near here)

4.4. Singlet oxygen determination

A tentative mechanism involving O_2 in the photolysis of CT is the formation of $^1O_2$ via energy transfer from the T_1 excited state as is shown in Scheme 1, where the last equation shows the indirect method used to prove the presence of $^1O_2$.

(Scheme 1 near here)

L-cysteine in the presence of $^1O_2$ forms L-cystine through a soft oxidation forming a disulfide bridge. A solution of CT/L -cysteine was irradiated in the presence of O_2 and the formation of a white solid was observed. The control reaction in darkness did not present solid formation. In order to identify this solid, L-cystine was synthezised via a

soft oxidation of L-cysteine. The formation of the same white solid was observed as well.

The solids were recovered via filtration, dried and analyzed through IR spectroscopy (see sup. inf. Figure S8). Also, the IR spectrum of L-cysteine was obtained. The spectra for the solid obtained in the photolysis and in the synthesis were identical while the spectrum of L-cysteine was different. We can conclude that the formation of L-cystine in the photolysis is due to the presence of $^1O_2$ in the solution, produced by the deactivation of the excited state (T_1) of CT.

4.5. Photoproducts analysis

The photolysis of **1** in ACN was fulfilled and the crude was analyzed via GC-MS and ^{1}H NMR to elucidate the identity of the photoproducts. From the results obtained we proposed the mechanism shown in scheme 2 together with the relative percentages of the photoproducts.

(Scheme 2 near here)

According to the products determined, we believe that in the presence of O_2, three possibilities are active, resulting in the reductive dechlorination (A and B) or reductive decyanation (C) of **1**. The most abundant photoproduct was 2,4,6-trichloroisophtalonitrile **2** formed through pathway **A**, while the less abundant one was 2,3,4,6-tetrachlorobenzonitrile **4** (pathway **C**). To the best of our knowledge, this is the first time where the speciation between isomers is informed and confirmed through GC/MS and NMR techniques. Another outcome was that no secondary photoproducts were observed.

On the other hand, the photolysis of **1** in N_2 gave the same primary photoproducts (pathways **A**, **B** and **C**); however, other pathways were opened allowing the formation of products resulting either from a reductive dechlorination (compounds **5a** to **d**) or decyanation (compounds **6a**,**b**). By comparing the relative percentages of the photoproducts it is possible to see that though there is a leveling in the amount of **2** and an increase of **3** in deoxygenated solution in respect to the oxygenated one, **4** shows an important decrease. This likely means that **4** is readily photolized giving the secondary photoproducts **6a** and **6b**.

In order to determine the identity of the different isomers (**2** and **3**; **5a-d**, and **6a**,**b**) a preparative photolysis in N_2 was performed. Via preparative chromatography we were able to separate the products into 3 fractions which were then analyzed by GC-MS and ^{1}H NMR. Nevertheless, the amount obtained were only adequate to uniquely characterize compounds **2**, **3**, **5a** and **5b** by both techniques, while all the others were characterized only by GC-MS.

5. Conclusions

The UV spectrum of CT in different solvents (acetonitrile, ethanol and a mixture of acetonitrile:water (70:30)) was measured and the vibrationally resolved spectrum for the HOMO→LUMO transition, using the Franck-Condon approximation, is presented for the first time. The spectrum shows remarkable agreement for both, absorption and fluorescence excitation.

Though the present paper used shorter wavelength irradiation than the vast majority of papers informed, leaving originally the molecule in its second excited state (S_2), it is concluded that non radiative processes very efficiently take the molecule to the lowest excited state (S_1) giving outcomes similar to those found in other papers.

Also, a detailed study of the photoproducts showed that in the presence of oxygen only the first reductive dechlorination-decyanation occurred, while in its absence a successive dechlorination-decyanation takes place.

Acknowledgements

Thanks are due to CONICET, SECYT and FONCYT for financial support. M. V. C. acknowledges a PhD fellowship from CONICET. Special thanks go to Mr. Alfredo Sattler from ADAMA S.A. for providing us the chlorothalonil samples. This work used Mendieta Cluster from CCAD-UNC, which is part of SNCAD-MinCyT, Argentina.

7. References

1 V. A. Sakkas, D. A. Lambropoulou and T. A. Albanis, *Chemosphere*, 2002, **48**, 939-945.

2 M. E. DeLorenzo and M. H. Fulton, *Marine Pollution Bulletin*, 2012, **64**, 1291-1299.

3 L. P. Gianessi, C. S. Silvers, *National Center for Food and Agricultural Policy, Trends in crop pesticide use: comparing 1992 and 1997*, **2000**.

4 H. Bessi, C. Cossu-Leguille, A. Zaid and P. Vasseur, *Bull. Environ. Contam. Toxicol.*, 1999, **63**, 582-589.

5 E. P. Gallagher, R. C. Cattley, and R. T. DiGiulio, *Chemosphere*, 1992, **24**, 3-10.

6 *Phytosanitary products guide for Argentina*, **2005**, Agricultural and Fertilizers Health Chamber (CASAFE), Argentina.

7 P. Y. Caux, R. A. Kent, G. T. Fan and G. L. Stephenson, *Crit. Rev. Environ. Sci. Technol.*, 1996, **26**, 45-93.

8 M. Millet, W. U. Palm and C. Zetzsch, *Ecotoxicol. Environ. Saf.*, 1998, **41**, 44-50.

9 G. A. Peñuela and D. Barcelo, *J. Chromatogr. A*, 1998, **823**, 81-91.

10 J. W. Kwon and K. L. Armbrust, *J. Agric. Food Chem.*, 2006, **54**, 3651-3657.

11 Y. Q. Tan, H. X. Xiong, T. Z. Shi, R. M. Hua, X. W. Wu, H. Q. Cao, X. D. Li and J. Tang, *J. Agric. Food Chem.*, 2013, **61**, 5003-5008.

12 S. U. Khan and M. H. Akhtaar, *Pestic. Sci.*, 1983, **14**, 354-358.

13 P. Dureja and S. Walia, *Toxicol. & Environ. Chem.*, 1993, **37**, 215-220.

14 A. G. Giumanini, G. Verardo and P. Strazzolini, *J. Photochem. Photobiol. A*, 1989, **48**, 129-153.

15 S. Samanta, R. K. Kole, L. K. Ganguly and A. Chowdhury, *Bull. Environ. Contam. Toxicol.*, 1997, **59**, 367-374.

16 R. W. Binkley, G. L. Kirstner, V. C. Opaskar and P. Olynyk, *Chemosphere*, 1977, **4**, 163-166.

17 S. Monadjemi, M. El Roz, C. Richard and A. Ter Halle, *Environ. Sci. Technol.*, 2011, **45**, 9582-9589.

18 S. Bouchama, P. de Sainte-Claire, E. Arzoumanian, E. Oliveros, A. Boulkamh and C. Richard, *Environ. Sci.: Processes Impacts*, 2014, **16**, 839-847.

19 M. G. Sarmiento Tagle, M. L. Salum, E. I. Buján and G. A. Argüello, *Photochem. Photobiol. Sci.*, 2005, **4**, 869-875.

20 M. V. Cooke, I. Malvacio, W. J. Peláez, A. J. Pepino, M. R. Mazzieri and G. A. Argüello, *RSC Adv.*, 2015, **5**, 26255-26262.

21 M. J. Frisch, G. W. Trucks, H. B. Schlegel, G. E. Scuseria, M. A. Robb, J. R. Cheeseman, G. Scalmani, V. Barone, B. Mennucci, G .A. Petersson, H. Nakatsuji, M. Caricato, X. Li, H. P. Hratchian, A. F. Izmaylov, J. Bloino, G. Zheng, J. L. Sonnenberg, M. Hada, M, Ehara, K. Toyota, R. Fukuda, J. Hasegawa, M. Ishida, T. Nakajima, Y. Honda, O. Kitao, H. Nakai, T. Vreven, J. A. Montgomery Jr., J. E. Peralta, F. Ogliaro, M. Bearpark, J. J. Heyd, E. Brothers, K. N. Kudin, V. N. Staroverov, R. Kobayashi, J. Normand, K. Raghavachari, A. Rendell, J. C. Burant, S. S. Iyengar, J. Tomasi, M. Cossi, N. Rega, J. M. Millam, M. Klene, J. E. Knox, J. B. Cross, V. Bakken, C. Adamo, J. Jaramillo, R. Gomperts, R. E. Stratmann, O. Yazyev, A. J. Austin, R. Cammi, C. Pomelli, J. W. Ochterski, R. L. Martin, K. Morokuma, V. G. Zakrzewski, G. A. Voth, P. Salvador, J. J. Dannenberg, S. Dapprich, A. D. Daniels, Ö. Farkas, J. B. Foresman, J. V. Ortiz, J. Cioslowski and D. J. Fox, *Gaussian 09 Revision E.01*. Gaussian Inc. Wallingford CT 2009.

22 A. D. Becke, *J. Chem. Phys.*, 1993, **98**, 5648-5652.

23 C. Lee, W. Yang and R. G. Parr, *Phys. Rev. B*, 1988, **37**, 785-789.

24 V. Barone and M. Cossi, *J. Phys. Chem. A*, 1998, **102**, 1995-2001.

25 M. Cossi, N. Rega, G. Scalmani and V. Barone, *J. Comput. Chem.*, 2003, **24**, 669-681.

26 J. Bloino, Development and Application of time dependent and time independent models for the study of spectroscopic properties in compounds of biological interest. Tesi di dottorato, Università degli studi di Napoli Federico II, 2008.

27 V. Barone, J. Bloino, M. Biczysko and F. Santoro, *J. Chem. Theory Comput.*, 2009, **5**, 540-554.

28 J. Bloino, M. Biczysko, F. Santoro and V. Barone, *J. Chem. Theory Comput.*, 2010, **6**, 1256-1274.

29 F. Duschinsky, *Acta Physicochimica U.R.S.S.*, 1937, **7**, 551-566.

30 H. Baumann, R. E. Martin and F. Diederich, *J. Comput. Chem.*, 1999, **20**, 396-411.

31 J. Franck, *Trans. Faraday Soc.*, 1926, **21**, 536-542.

32 E. U. Condon, *Phys. Rev.*, 1928, **32**, 858-872.

33 V. Barone, J. Bloino and M. Biczysko, *GAUSSIAN 09 Revision A.02*, 2009, 1-20.

34 F. Muniz-Miranda, A. Pedone, G. Battistelli, M. Montalti, J. Bloino and V. Barone, *Journal of Chemical Theory and Computation*, 2015, **11**, 5371-5384.

35 G. Pietraperzia, M. Pasquini, F. Mazzoni, G. Piani, M. Becucci, M. Biczysko, D. Michalski, J. Bloino and V. Barone, *J. Phys. Chem. A*, 2011, **115**, 9603-9611.

36 N. Schiccheri, M. Pasquini, G. Piani, G. Pietraperzia, M. Becucci, M. Biczysko, J. Bloino and V. Barone, *Phys. Chem. Chem. Phys. PCCP*, 2010, **12**, 13547-13554.

37 H. Wang, Y. Liu, M. Li, H. Huang, H. M. Xu, R. J. Hong and H. Shen, *Optoelectron. Adv. Mat. Rapid Communications*, 2010, **4**, 1166-1169.

38 M. Biczysko, J. Bloino and V. Barone, *Chem. Phys. Lett.*, 2009, **471**, 143-147.

39 A. M. Brouwer, *Pure Appl. Chem.*, 2011, **83**, 2213-2228.

40 J. Porras, J. J. Fernández, R. A. Torres-Palma and C. Richard, *Environ. Sci. Technol.*, 2014, **48**, 2218-2225.

Figures, tables and schemes

Figure 1. UV spectra of CT in ACN **[a]** and amplification of the medium **[b]** and long **[c]** wavelength regions

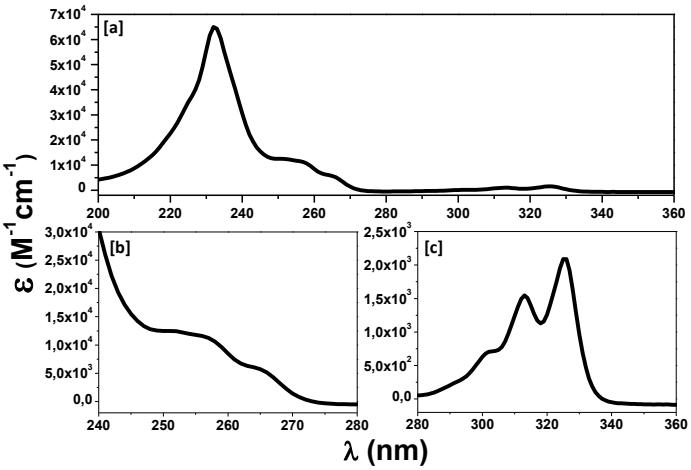

Table 1. λ_{max} (nm) and ε ($M^{-1}cm^{-1}$) of CT in different solvents

Solvent		
ACN	EtOH	H_2O:ACN (70:30)
224 (33300)	225 (32520)	225 (33840)
232 (67200)	233 (58600)	233 (66400)
258 (11320)	258 (11240)	259 (11560)
266 (5650)	266 (6250)	267 (6170)
301 (850)	301 (764)	301 (1040)
313 (1760)	313 (1645)	314 (2000)
326 (2310)	326 (2207)	327 (2590)

Figure 2. Absorption spectrum of CT in ACN and transitions calculated by TD-DFT/B3LYP/6-31+G(d,p).

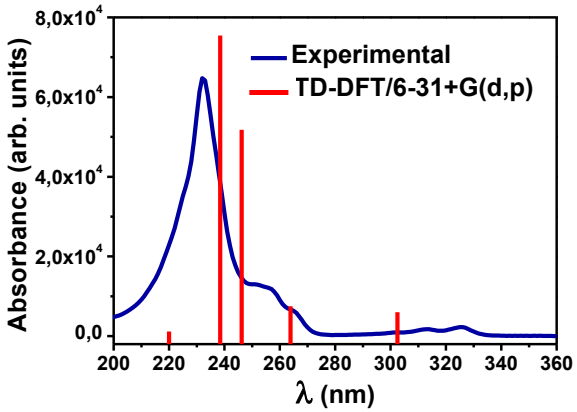

Figure 3. Representation of the relevant HOMOs and LUMOs and TD-DFT calculated transitions, oscillator strength, calculated molar absorption coefficient and assignment of CT in ACN.

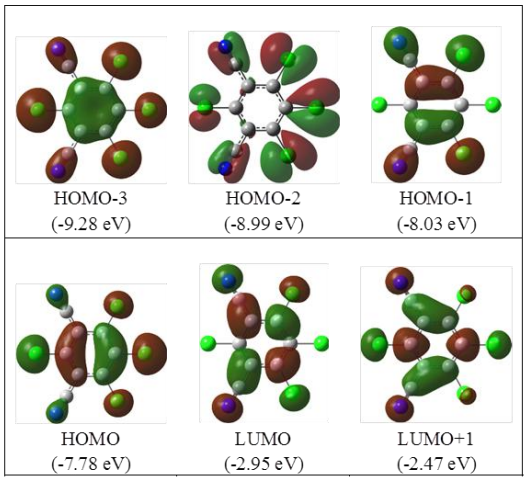

Calculated (TD-DFT)[a]			Transition[b]	Assignment
λ_{max}^{calc}	F	ε_{calc}		
220.0	0.0114	769	H-3→L+1(98%)	π→π*
238.5	0.7452	50282	H-1→L+1(79%) H→L(19%)	π→π*
246.2	0.5116	34520	H→L+1(74%) H-1→L(23%)	π→π*
263.9	0.0740	4993	H-1→L(75%) H→L+1(24%)	π→π*
302.5	0.0595	4015	H→L(80%) H-1→L+1(20%)	π→π*

[a]TD-B3LYP 6-31+G(d,p).

[b]H-highest occupied MO (HOMO), L-lowest unoccupied MO (LUMO).

Figure 4. Vibrationally resolved absorption spectrum with active vibronic transitions for CT.

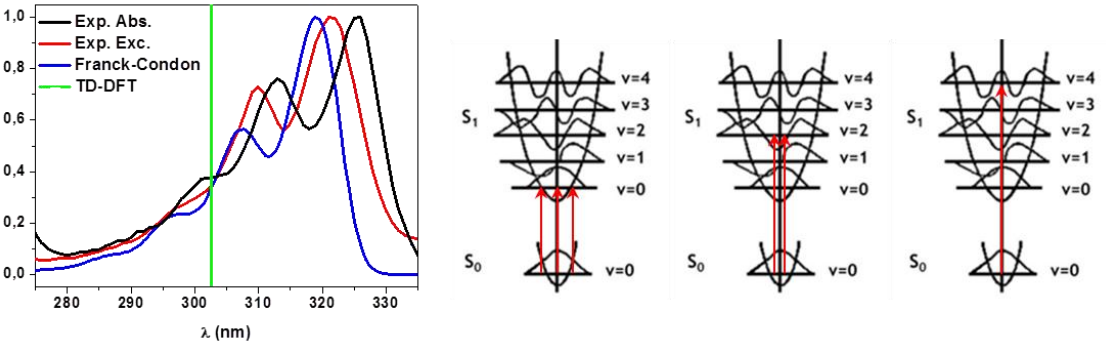

Figure 5. Photolysis of CT followed via UV spectroscopy (solid lines) and emission fluorescence spectrum for excitation at 254 nm (dashed line). Time is given in minutes.

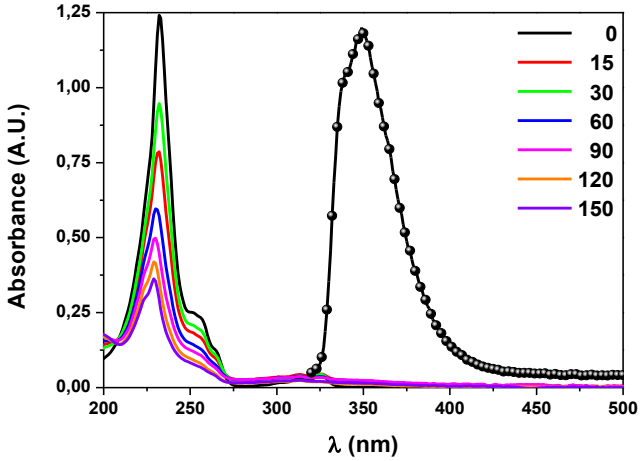

Figure 6. ln(A/A$_0$) vs time of CT in O_2 and N_2 environments. Inset: Overall constants of the photolysis of CT in the presence and absence of O_2 and their ratio

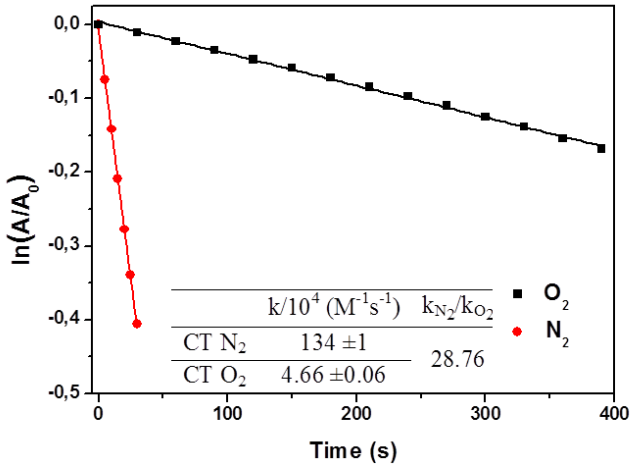

Scheme 1. Proposed reaction mechanism

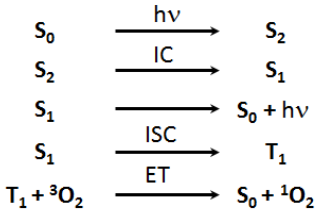

Indirect detection of $^1O_2$

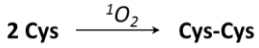

Scheme 2. Proposed Mechanism for CT and relative percentages of the photoproducts of **1** in O_2 and N_2 environment

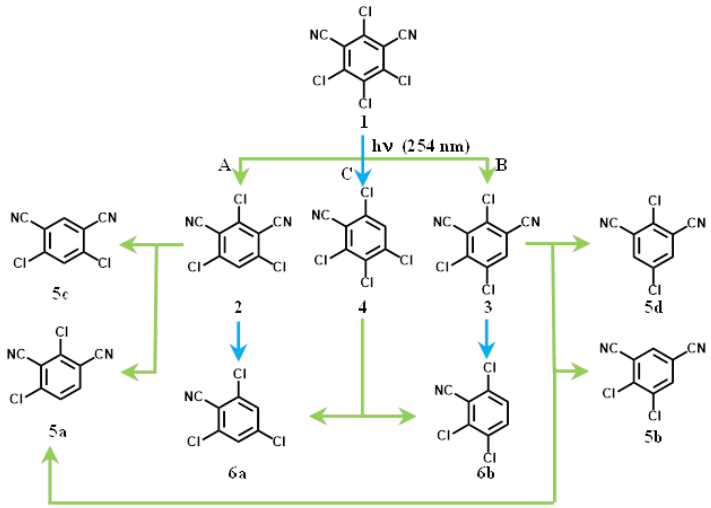

Prod. (%)	2	3	4	5a	5b-d	6a	6b
Rt (min)	6.89	7.08	6.35	5.55	5.36 5.64 6.07	4.71	5.22
O_2	75.4	14.5	10.1	-	-	-	-
N_2	69.8	20.0	5.2	1.7	1.5	1.3	0.5

Supplementary Material

Click here to download Supplementary Material: Supporting Information.docx